PROCEEDINGS OF SCIENCE

Operation of the OPPIS H⁻ Ion Source during the RHIC Run-2024

A. Cannavo',* G. Atoian, D. Raparia,* T. Lehn, J. Ritter, B. Snyder and A. Zelenski

Brookhaven National Laboratory,
Upton, New York, USA

E-mail: acannavo@bnl.gov, raparia@bnl.gov

This work provides an overview of the operation of the Optically Pumped Polarized Ion Source (OPPIS) during the polarized proton Run-24 of the Relativistic Heavy Ion Collider (RHIC). The successful performance of the source was achieved through targeted upgrades focusing on three key aspects: performance, stability, and safety.
The modifications to the Na-cell optimized the collection of Na vapors, extending the operational duration of the cell to over six months without requiring refilling of the Na reservoir. Similarly, changes to the plasmatron significantly increased the lifetime of source components, ensuring consistent and uninterrupted beam current throughout the run. A novel concept was implemented for the Rb cell, which showed promising preliminary results but did not result in an increase in the average polarization.
A 10 % enhancement in beam transport efficiency was achieved by the modifications of the Low Energy Beam Transport (LEBT).
The upgrades enabled reliable operation throughout Run-24, delivering a mean 350 µA and 300 µs beam current with an average 80 % polarization at the output of the 200 MeV linac. Finally, an extended beam width of 420 µs was successfully tested with minimal polarization losses, leading to the injection of 1×10^{12} protons into the Booster.

PSTP2024,
22-27 September 2024
Jefferson Lab Newport News, VA

*Speaker

PoS(PSTP2024)006

1. Introduction

The 24th run of the Relativistic Heavy Ion Collider (RHIC) was marked by significant technological upgrades aimed at enhancing collision rates, data acquisition, and overall operational efficiency. Among the key improvements were the skew quadrupole upgrade for the AGS, designed to reduce polarization loss from horizontal resonances [1], and the commencement of physics data taking with the newly commissioned sPHENIX detector [2]. Proton-proton collisions during this run served to explore proton spin, Quark Gluon Plasma, establish baseline data for future gold-gold collisions, and gain operational experience ahead of the transition to the Electron-Ion Collider (EIC). To meet the demands and objectives of this run, the Optically Pumped Polarized Ion Source (OPPIS) received extensive upgrades, with improvements made to all important components. This paper provides a description of the modifications, and a summary of the OPPIS performance and achievements within the Run-24.

2. OPPIS Source

The proton polarization techniques of the OPPIS, thoroughly explained in [3–5], can be summarize into four main blocks:

1. Fast Atomic Beam Source (FABS).
2. Superconducting Solenoid region (SCS).
3. Sona Transition region.
4. Na-jet ionizer and extraction.

2.1 Fast Atomic Beam Source (FABS)

The FABS consists of an arc discharge plasma ion source (plasmatron), a 4-grid extractor, and a hydrogen cell neutralizer. Hydrogen gas is injected into the plasmatron via a pulsed valve where the arc discharge produces the plasma. The plasma flows through the arc discharge channel, which is composed of isolated metallic diaphragms, and exits through the anode aperture. As the plasma expands into the vacuum without collisions, the ion component undergoes cooling because of the phase space conservation [6]. The proton beam is then produced by the spherically shaped 4-grid Ion Optical System, that provides with ballistic beam focusing (with a focal length of about 200 cm) and eventually is neutralized in the H-cell with 90% efficiency. The FABS produces an atomic hydrogen beam with an intensity of approximately 3 A at a beam energy of 6-8keV.

2.2 Superconducting solenoid (SCS) region

The atomic beam enters the 2.5 T magnetic fields of the Superconducting Solenoid (SCS), where it is partially ionized to protons in the pulsed He-cell, with an efficiency of about 60-70%. The high voltage bias is applied to the He-cell grid system which decelerates protons to 4 keV, while the non-ionized part of the beam retains its energy of 6-8 keV. In the Rb-cell the ionized beam picks up optically pumped polarized electrons (70% efficiency) from the Rb evaporation cloud to form a neutral beam of electron-spin polarized hydrogen atoms. Deflector plates downstream of the Rb-cell remove any remaining charged particles.

2.3 Sona transition region

The electron-polarized hydrogen beam passes through a magnetic field reversal region, where polarization is transferred to the nucleus through hyperfine interaction according to the so-called Sona-transition method [7]. A system of correction coils allows to tune the profile of the longitudinal magnetic field to satisfy the adiabatic condition and the sudden zero-field crossing to prevent polarization loss.

2.4 Na-jet ionizer and extraction

The atoms are then negatively ionized with an efficiency of about 8% by a Na-jet vapor in a 0.15 T magnetic field. Eventually the beam is extracted to form nuclear-polarized and unpolarized H^- ions at 30 keV and 36 keV, respectively. Further suppression of the unpolarized component occurs in the Low Energy Beam Transport (LEBT) line and the RFQ shown in Fig. 3. The unpolarized beam is well separated after passing through a 23.7° bend and a system of collimators in the LEBT; additional suppression in the RFQ nearly eliminates the unpolarized component down to ~3 %. The spin direction is changed from longitudinal to horizontal polarization direction by the 23.7° bend and then to the vertical direction by the so-called Spin Rotator.

3. Development of the source

The development of the source was strategically guided by three fundamental principles: enhancing performance, ensuring long-term stability, and maintaining the highest safety standards.

3.1 Cathode

The cathode geometry was modified by adding a small nozzle and doubling the thickness of the outer rim d=3.2 mm (Fig.1). The new nozzle's design allows for more efficient shaping of the puffed gas as it enters the discharge channel, leading to a more uniform wear pattern on the cathode as can be seen in the comparative picture Fig. 1 before (first column) and after (second column).

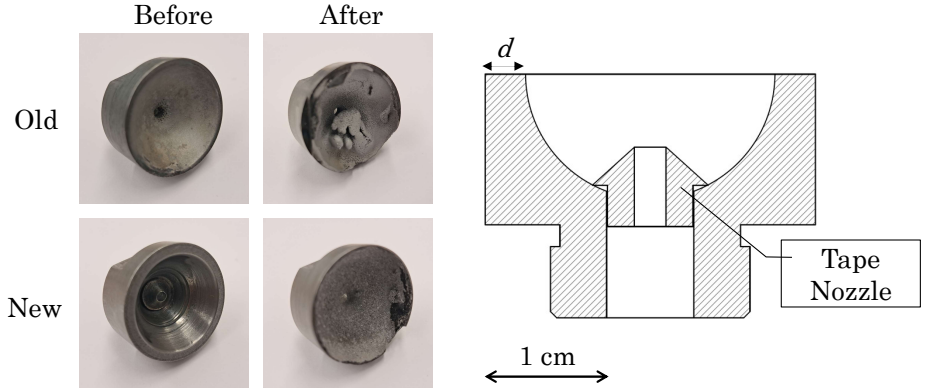

Figure 1: On the first column, cathodes before installation in the source with new (top) and old (geometry), and their corresponding wear after (second column); a section of the new cathode geometry.

Additionally, the vacuum sealing of the valve assembly was enhanced, effectively minimizing hydrogen dispersion within the plasmatron. These improvements had a significant impact on the

cathode's lifetime, as the typical blistering and clustering effects were not observed in the modified cathode. While the previous cathode had an average lifetime of about two months, the current plasmatron assembly has operated for an extended period of 29 weeks. Although the cathode exhibited no signs of performance degradation, it was replaced to ensure continued operation throughout the extended duration of the run.

3.2 Rb cell

A new design concept for the Rb cell was used for the Run-24. Unlike the original design (left of Fig. 2a), where the liquid Rb reservoir channel was directly open to the beam channel, the updated design (right of Fig. 2a) distributes Rb across an outer stainless-steel vessel and the Rb vapor uniformly diffuses into an inner copper cylinder through four lateral slits (Fig. 2c).

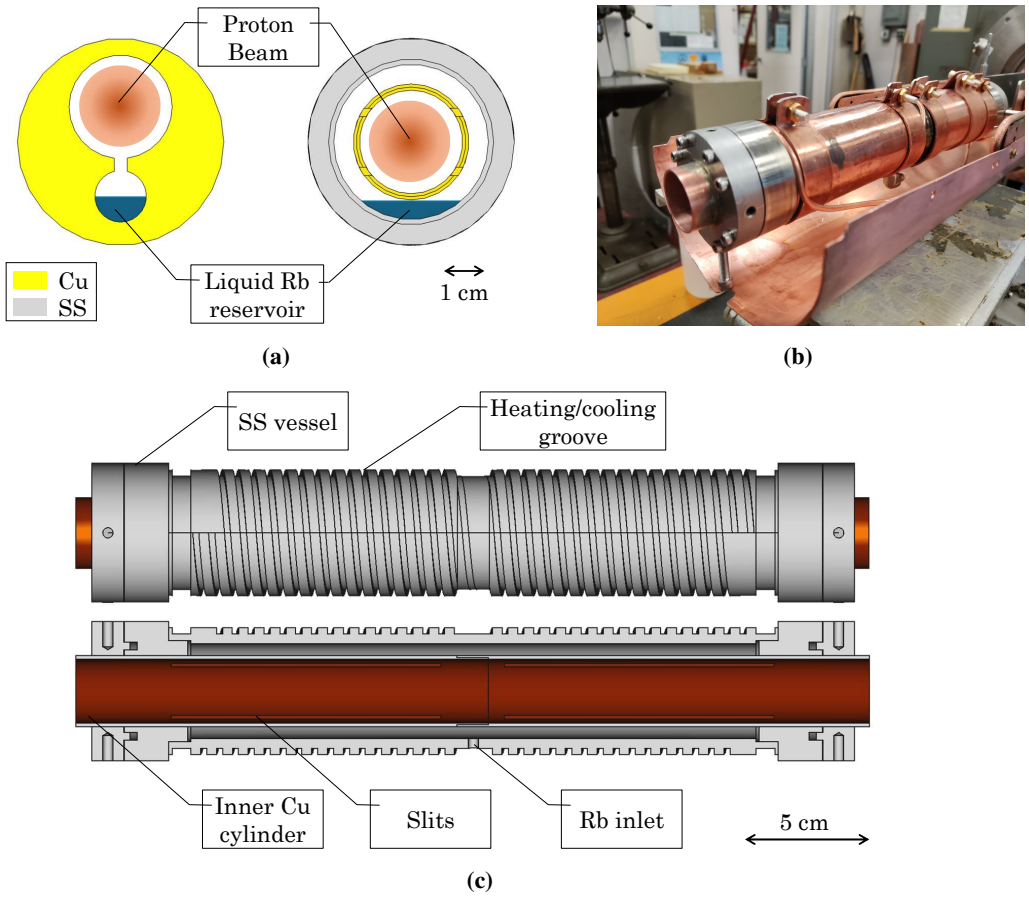

Figure 2: (a) Sections of the two different concepts of the Rb-cell; photo (b) and sketch (c) of the newly designed Rb-cell assembly.

The larger longitudinal size of the slits extends the region with homogeneous Rb vapor distribution, enabling operation at lower Rb vapor density. To improve temperature control, an additional groove was added to the outer stainless-steel vessel for the cooling line (Fig.2c), and a copper shield was implemented on top of the SS vessel to ensure uniform temperature distribution throughout the cell (Fig. 2b). The system has proven stable at standard operational temperature thanks to the

balanced heating and cooling lines. No special maintenance requiring the removal of the cell from the vacuum was needed. An advantage of the new design is its possibility to be fully dismantled, eliminating enclosed small-volume gaps where Rb could accumulate. This improvement makes the cleaning process after run both safer and faster. However, a bed connection of the read-back thermocouple was responsible for a slow reaction of the feedback system leading to an extended temperature transient ($\sim$ 1 h) during the heating ramp.

3.3 Na-jet ionizer

The changes performed on the Na-cell concern the Na reservoir container and the collector cooling line. The Na container volume was reduced from 500 to 230 mL and heater thermal coupling to reservoir was also improved. The installation of a water pressure regulator in the collector cooling line allowed to insulate the collector from pressure instability of the local cooling system. This, in turn, stabilized the collector temperature that benefits the stability of sodium circulation. The result of these changes was a prolonged operation time of the Na-jet ionizer, greater than 6 months without refilling the Na reservoir.

4. LEBT modifications

The LEBT (Fig. 3) serves as the connecting section between the high-intensity magnetron sources, the OPPIS and the 750 keV RFQ. This run benefited from LEBT modifications implemented earlier in 2022. Specifically, the distance between the Na-jet ionizer and the 23.7° dipole magnet was reduced by approximately 2 m. Additionally, the electrostatic Einzel lenses were replaced with magnetic quadrupole lenses.

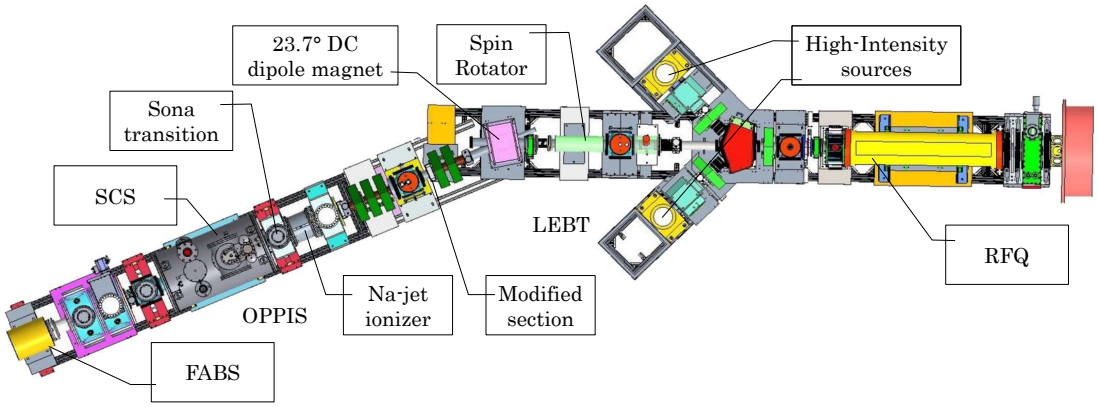

Figure 3: Updated layout of the LEBT

Due to yearly variability in source parameters, run-to-run comparisons to quantify the exact improvements achieved by these changes are somewhat challenging. However, according to the best estimates [8], the modifications have resulted in an overall 10 % enhancement, attributed to reduced beam losses caused by space charge effects. Moreover, the reduced length had a positive impact on the transport of the pumping laser beam.

5. Run Overview and achievements

Fig. 4a and Fig. 4b show the run overview of the current and polarization, respectively, as measured after the 200 MeV linac. The robust construction of the OPPIS, as demonstrated in previous runs, ensured uninterrupted operation throughout the entire duration of this run.

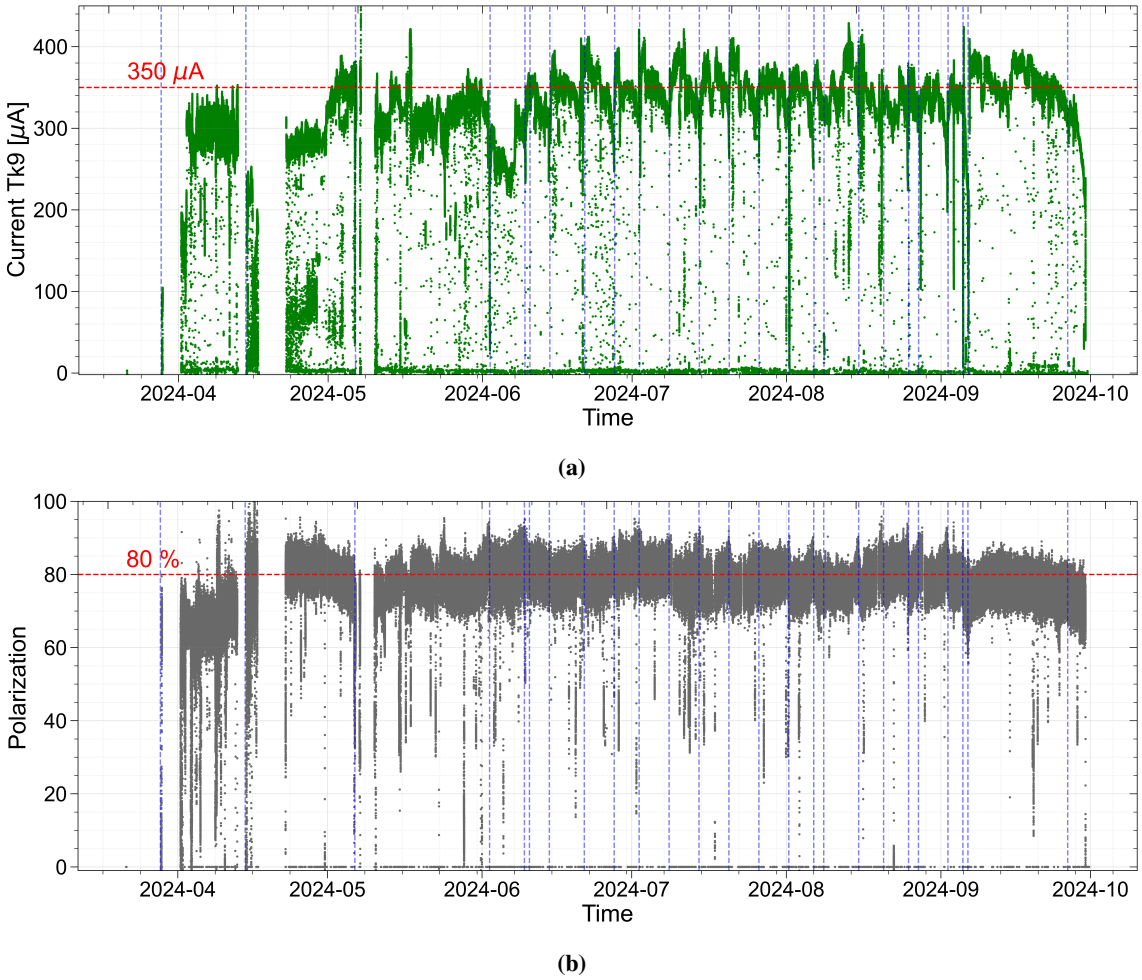

Figure 4: Overview of the current (a) polarization (b) as measured after the 200 MeV linac; blue lines show the filling procedures of the Rb-cell.

The two interruptions occurred in April and May were not directly related to the source malfunctions. The typical beam current delivered after the linac was approximately 350 µA for a 300 µs pulse, corresponding to a booster input of 6.3×10^{11} protons per bunch. This value is consistent with typical performance in previous years. During this run we also tested the possibility of beam pulse duration extension. The test demonstrated the stability of the beam at an extended width of 420 µs enabling a 40 % increase in the total number of ions injectable in the Booster. Through fine-tuning of the source and beam transport line, a stable 8 h operation with a peak value of 1×10^{12} protons per bunch was achieved with a 400 µA and 400 µs beam. Fig. 5 presents a typical beam waveform

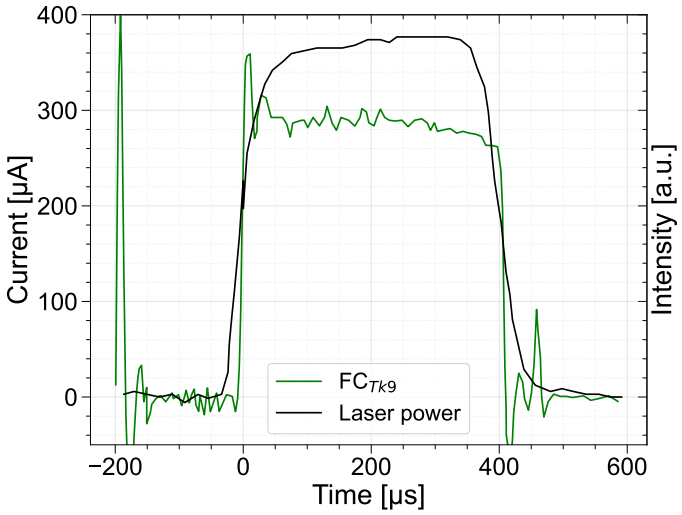

Figure 5: Extended beam pulse and laser power profile.

alongside the laser power profile. The design of the laser system limits the extendable time window to approximately 450 μs, beyond which significant polarization losses occur.

Fig. 4b points out that the average polarization during the Run-24 was around 78-80% and therefore no improvement was observed.

Indeed, the fluctuations in both current and polarization (Fig.4a, Fig. 4b) highlight a relationship between polarization and the amount of Rb in the SS vessel. Specifically, lower quantities of Rb corresponded to higher polarization levels and vice-versa. As a result, peak polarization values were achieved just before the Rb re-filling process, which is typically accompanied by a sudden drop in the beam current. To mitigate these fluctuations and achieve higher polarization level, the Rb filling strategy was adjusted: instead of monthly refills, more frequent fills with smaller amounts of Rb were implemented on a five-day cycle. Both Fig. 4a and Fig. 4b highlight the filling processes with blue dashed vertical lines. Despite the increased frequency, this adjustment did not affected operations, as the filling process is conducted without breaking the vacuum.

6. Conclusion

The results confirm that the developments efficiently improved performances, stability and safety of the Run-24 operations. The beam current of 350 μA satisfied the requirements for booster injection for an uninterrupted operational period of more than 6 months. The Run-24 gave also the opportunity to confirm an estimated 10 % enhancement of the beam transport efficiency achieved by shortening the LEBT line and replacing electrostatic Einzel lenses with magnetic quadrupole lenses. Stability was also consistently maintained with an average arcing rate as high as 2 %. It is worth mentioning that, while the He-cell presented the greatest challenge in terms of arcing (primarily due to the proximity of the HV grid to the Rb evaporation area), reliable operation was still achieved with beam pulse widths extending up to 450 μs thanks to the beneficial wire grids improvements in the beam deceleration system combined with a lower Rb vapor density. This demonstrates that the OPPIS system, including both the power supply and He grid system, can manage extended pulse

widths after proper conditioning. Moreover, as tested in an earlier study, the laser pulse width can also be extended to 500-600 µs with modification of the laser power supply. In terms of polarization, a lower average level was observed, likely attributable to the new Rb-cell design. During preliminary testing in preparation for Run-24, the new Rb-cell demonstrated higher polarization levels over short duration, which encouraged its final implementation. However, over extended operation, a strong correlation between polarization and the amount of Rb in the SS vessel became apparent through polarization measurements. While the exact cause is still under investigation, the leading hypothesis is that the increased longitudinal size of the Rb-cell leads to the formation of an extended Rb cloud. The size and shape of this cloud appear to vary dynamically and are highly dependent on the quantity of Rb in the vessel. Additionally, in attempt to obtain a longer homogeneous Rb vapor distribution using larger longitudinal slit size likely resulted in Rb penetrating lower-field regions, leading to polarization losses. If experimentally confirmed, these findings would provide valuable insights for the development of the next generation of Rb-cells.

Acknowledgment

This research is supported by Brookhaven Science Associates, LLC under Contract No. DE-SC0012704 with the U.S. Department of Energy.

References

[1] N Tsoupas, V Badea, S Belavia, H Huang, D Lehn, R Lynch, G Mahler, I Marneris, J Sandberg, V Schoefer, et al. A skew quadrupole for the AGS to minimize the polarization losses of the polarized beams. Technical report, Brookhaven National Lab.(BNL), Upton, NY (United States), 2022.

[2] E O'Brien. The construction of the sPHENIX detector and status of its commissioning. In *EPJ Web of Conferences*, volume 296, page 01007. EDP Sciences, 2024.

[3] Anatoli Zelenski. Polarized Ion Sources. In *Polarized Beam Dynamics and Instrumentation in Particle Accelerators: USPAS Summer 2021 Spin Class Lectures*, pages 245–260. Springer International Publishing Cham, 2022.

[4] A Zelenski. Review of Polarized Ion Sources. In *International Journal of Modern Physics: Conference Series*, volume 40, page 1660100. World Scientific, 2016.

[5] A Cannavo, G Atoian, T Lehn, D Raparia, J Ritter, B Snyder, and A Zelenski. High-intensity polarized and unpolarized H-sources development and operational at BNL. Technical report, Brookhaven National Laboratory (BNL), Upton, NY (United States), 2024.

[6] VI Davydenko. Formation of intense focused ion and atomic beams. *Nuclear Instruments and Methods in Physics Research Section A: Accelerators, Spectrometers, Detectors and Associated Equipment*, 427(1–2):230–234, May 1999.

[7] CS Kannis, R Engels, C Hanhart, H Soltner, L Huxold, K Grigoryev, A Lehrach, M Büscher, and T Sefzick. New Application of a Sona Transition Unit: Observation of Direct Transitions between Quantum States with Energy Differences of 10 neV and Below. In *Proceedings of the 24th International Spin Symposium (SPIN2021)*. Journal of the Physical Society of Japan, December 2022.

[8] D Raparia, J Alessi, G Atoian, and A Zelenski. Charge neutralized low energy beam transport at brookhaven 200 MeV linac. *Review of Scientific Instruments*, 87(2), 2016.